Overview of Measurements from the Wendelstein 7-X Stellarator Phase Contrast Imaging Diagnostic and Plans for the OP-2 Campaign*

Eric Edlund[1], Zhouji Huang[2], Miklos Porkolab[2], Søren Hansen[2], Adrian von Stechow[3],
Jan-Peter Bähner[3], Olaf Grulke[3], and the W7-X Team

[1]SUNY Cortland, Cortland, NY, USA
[2]MIT Plasma Science and Fusion Center, Cambridge, MA, USA
[3]Max-Planck-Institute for Plasma Physics, Greifswald, Germany

*Work of US Participants supported by the US DOE Grant DE-SC0014229

This work has been carried out within the framework of the EUROfusion Consortium and has received funding from the Euratom research and training programme 2014-2018 and 2019-2020 under grant agreement No 633053. The views and opinions expressed herein do not necessarily reflect those of the European Commission.

APS DPP virtual meeting, 11.9.2020, BP14.00005

Overview

- Overview of the W7-X stellarator
- Transport expectations: neoclassical versus turbulent transport
- Power balance in W7-X: the importance of turbulent transport
- Core turbulence diagnostics on W7-X: Phase Contrast Imaging (PCI)
- Profile shaping actuators and impact on turbulence and transport :

  (i) core fueling by cryogenic pellet injection and Electron Cyclotron Resonance Heating (ECRH)

  (ii) core Neutral Beam Injections (NBI) fueling

- Initial results of gyrokinetic simulations

The Wendelstein 7-X stellarator

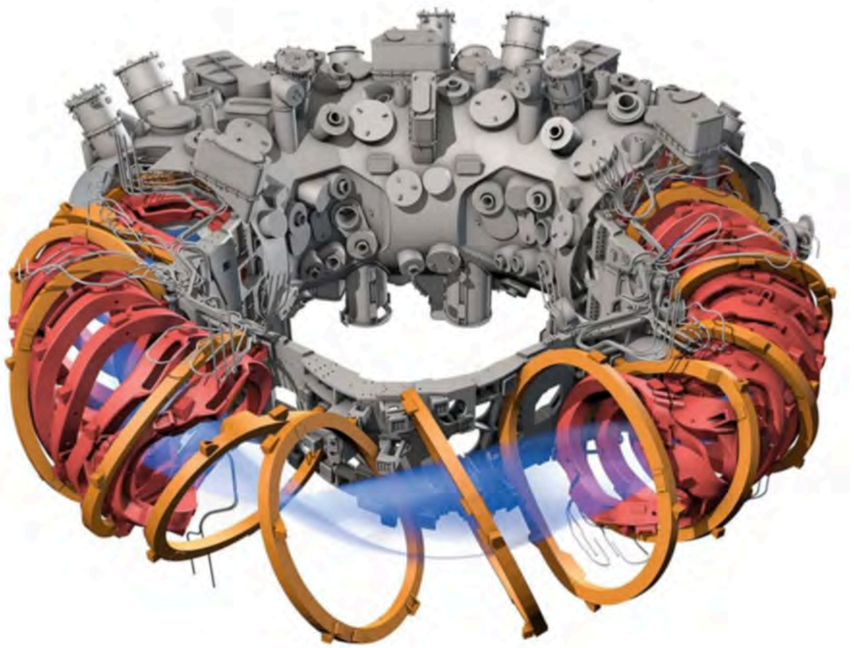

- **Modular coil stellarator** with variable magnetic configuration
- **B-field on axis:** 2.5T, rotational transform 5/6…5/4
- **Major/minor radius:** 5.5 m / 0.55 m
- **Plasma volume:** 30 m^3
- **Heating:** ECRH (< 7MW, steady state) and NBI (< 4 MW, O(10s))
- **Typical pulse lengths:** 5…100 s
- **Fueling:** gas valves, divertor nozzles and cryogenic pellets (+NBI)
- **Exhaust governed by island divertor** (carbon)
- **Turbulence optimization**

  Stabilizing effect for TEM due to averaging “good” and “bad” curvature regions along the orbit with a quasi-isodynamic configuration (maximum-J design, where J is the second adiabatic invariant)

Energy and particle transport in Wendelstein 7-X

$$D_e \sim \frac{\boxed{\epsilon_{\mathrm{eff}}^{3/2}}\, v_{\mathrm{d}}^2}{\nu_{\mathrm{e}}} \propto \frac{\epsilon_{\mathrm{eff}}^{3/2} T_{\mathrm{e}}^{7/2}}{n_{\mathrm{e}} B^2 R^2}$$

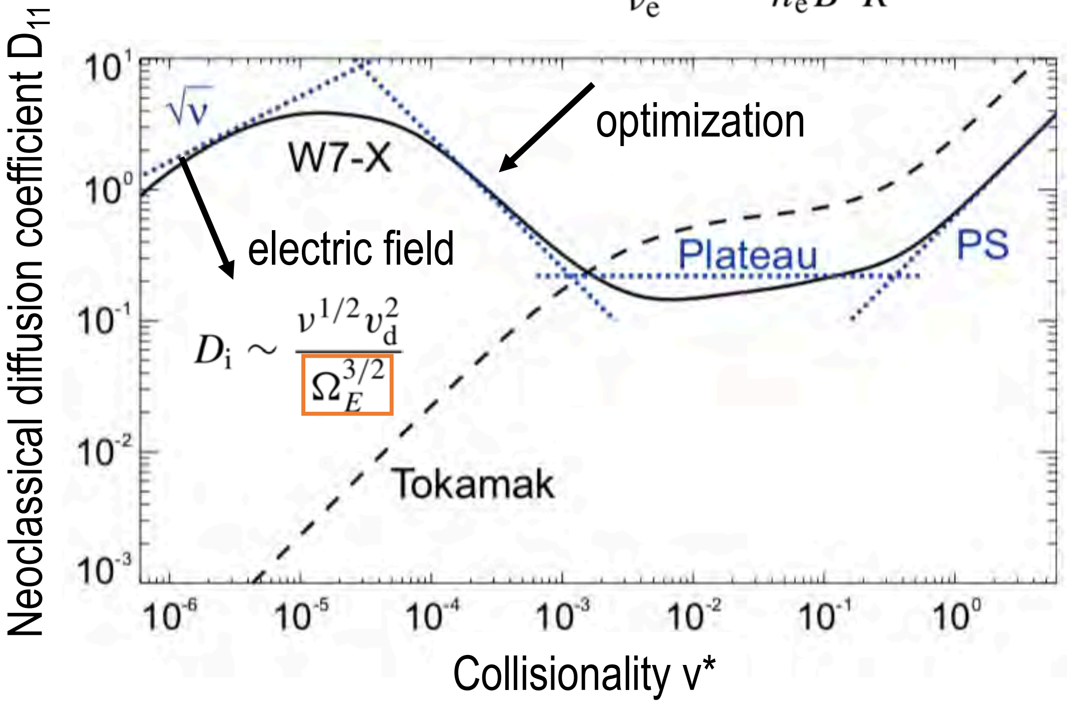

$$D_{\mathrm{i}} \sim \frac{\nu^{1/2} v_{\mathrm{d}}^2}{\boxed{\Omega_E^{3/2}}}$$

P. Helander, PPCF **54** (2012)

- In contrast to tokamaks, stellarators suffer from **enhanced neoclassical transport at low collisionality**
- **Diffusion scales with 1/v** at low collisionalities
- W7-X is designed to have **low neoclassical transport,** expressed by helical ripple ϵ_{eff}
- Operationally, **high densities are crucial**
- Additionally, **ExB rotation reduces diffusion** at lower collisionalities in the $\sqrt{\nu}$ regime
- NC transport optimization
  → **relative role of turbulence is increased**

Gyrokinetic predictions on W7-X

W7-X normal curvature at half radius (red: "bad")

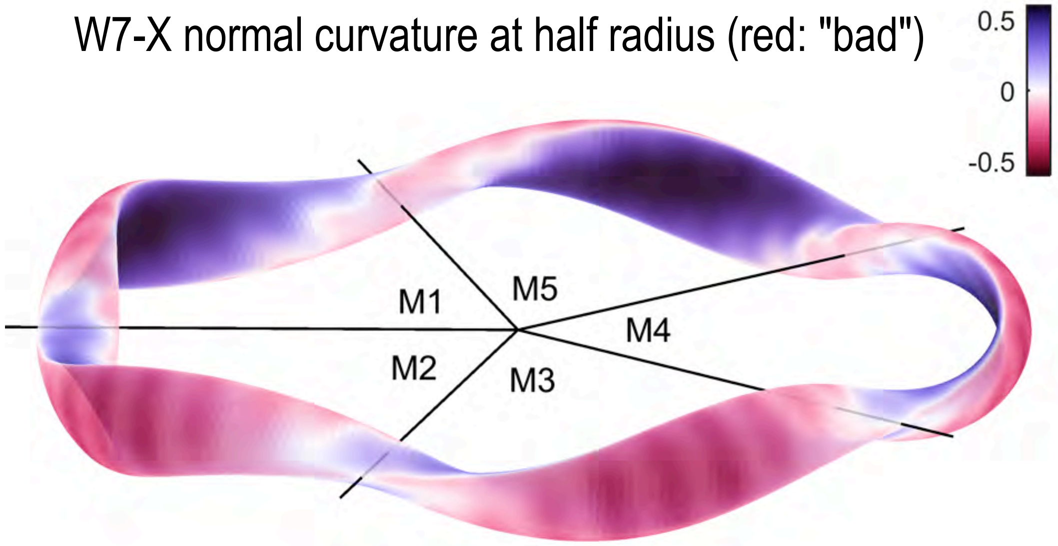

ITG density fluctuations on full flux surface

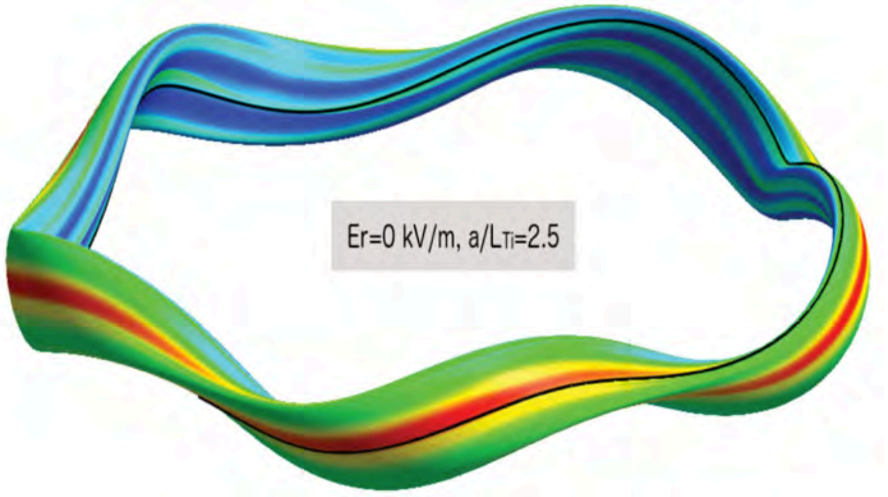

Xanthopoulos *et al.*, Phys. Rev. Lett. 125 (2020)

- Instability mechanisms: similar to Tokamak, but **curvature geometry is fundamentally different**
- ITG flux surface simulations: ”hot stripe” **poloidally and toroidally localized**
- Instabilities are sensitive to magnetic configuration and radial electric field
    - key parameters: elongation, mirror ratio, stellarator quasi-symmetries …

Heat and impurity transport in typical ECH discharges

T_i vs. T_e including peaked density profiles

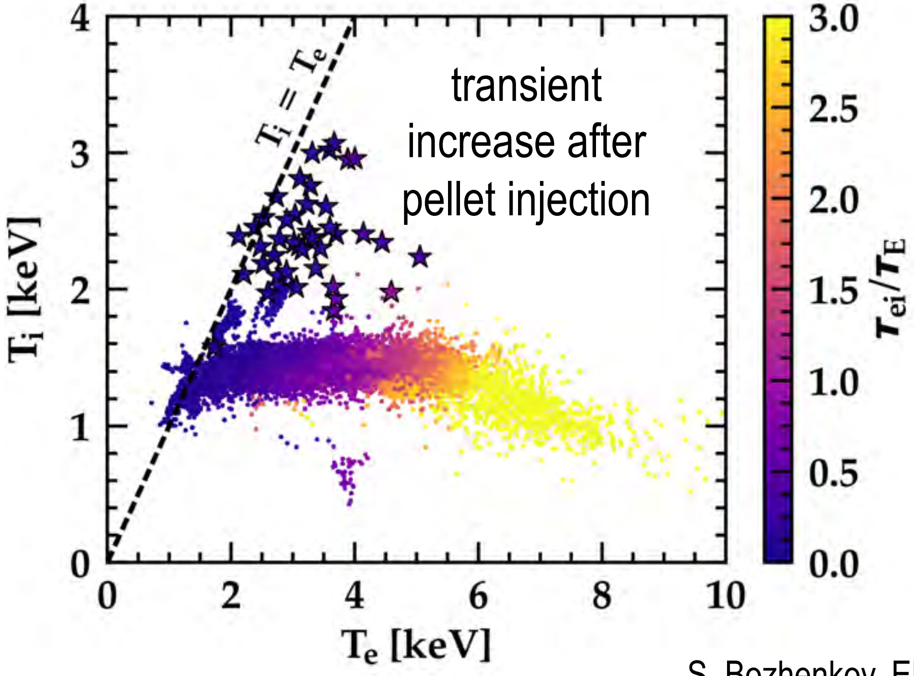

S. Bozhenkov, EPS 2019, Milan

injected impurity confinement times (laser blow-off)

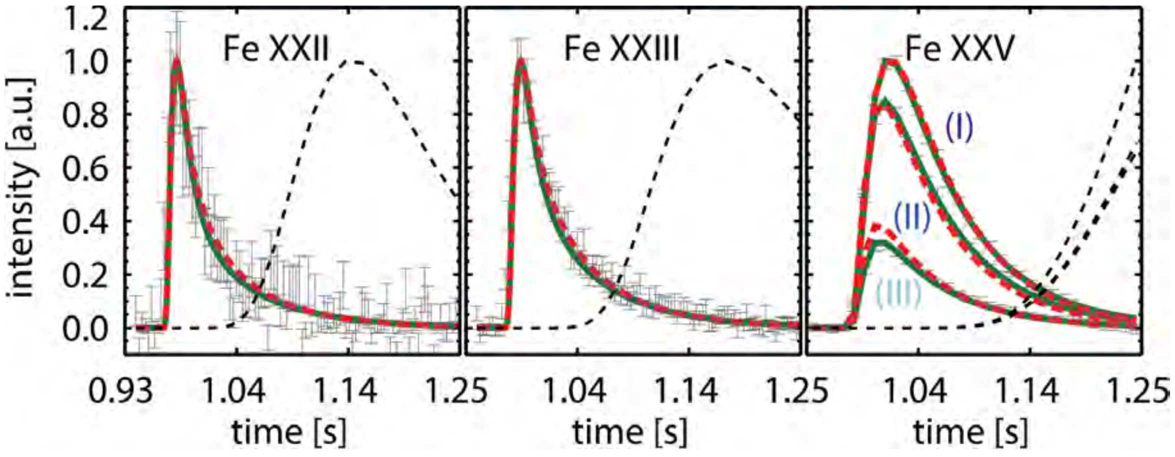

dashed: neoclassical prediction
red: prediction including anomalous diffusion

B. Geiger, NF **59** (2019)

- Full power balance (w/ ECRH power deposition, ion/electron flux and radiation profiles):
  → neoclassical terms fall short by a factor of ~10, indicating large anomalous heat transport
- Impurity confinement times cannot be modeled using neoclassical diffusion only
  → very large anomalous diffusion (>100x D_{NC}) required, indicating large anomalous impurity transport

Ion temperature limits in W7-X

power balance for flat density profiles

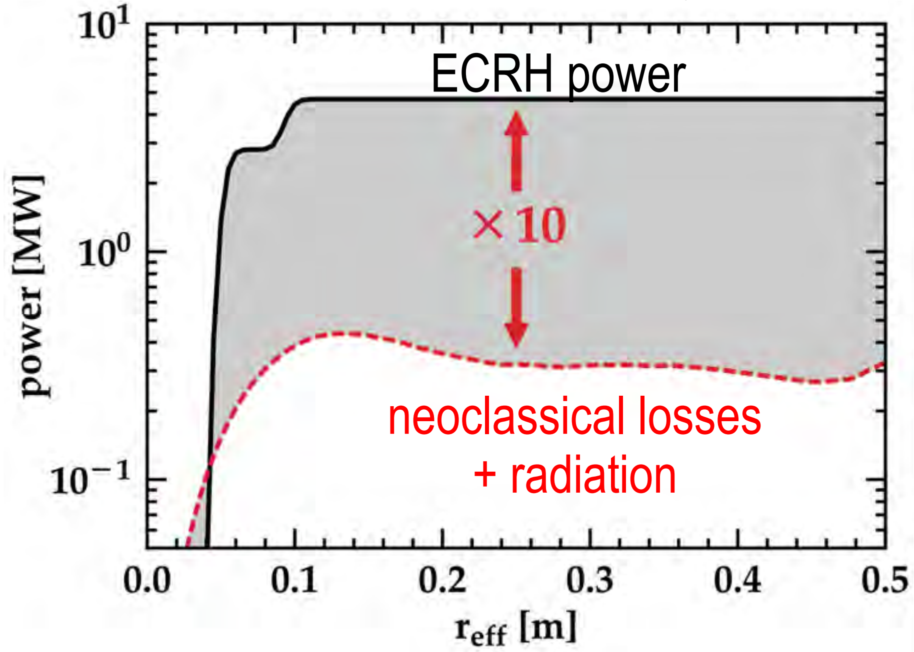

ECRH-heated, pellet-fueled

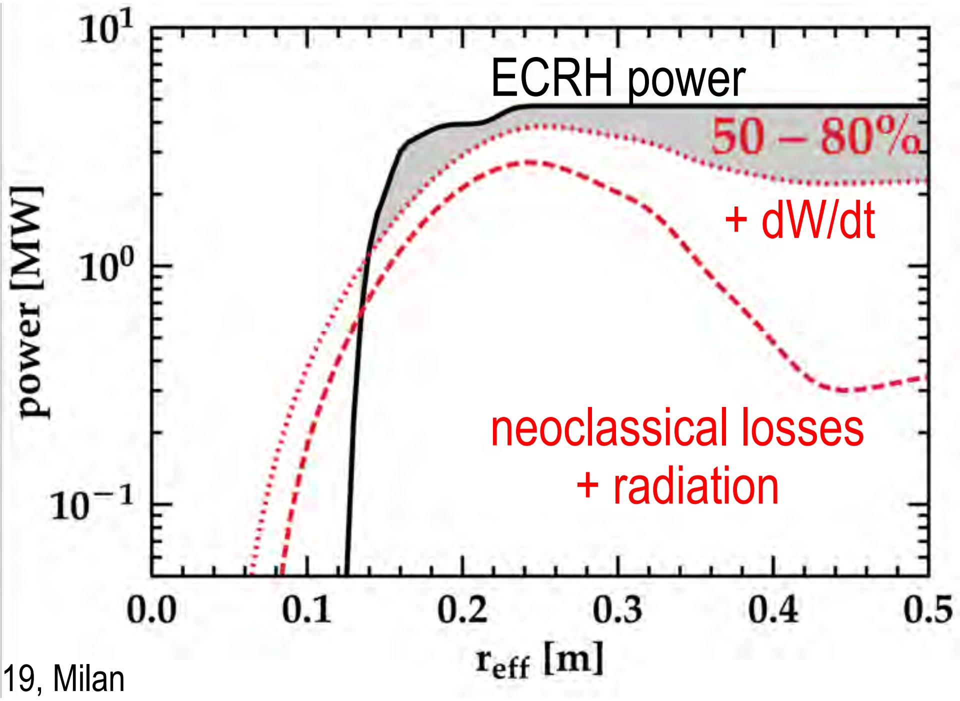

S. Bozhenkov, EPS 2019, Milan

- ECRH + flat density profiles: ion temperature limited to $T_i \lesssim 1.6$ keV in accessible n_e and P_{ECRH} parameter space
  - large shortfall compared to neoclassical expectations (w/ moderate anomalous losses)
- ECRH + peaked density profiles: highest W7-X ion temperatures and β achieved transiently w/ E_r transition to ion root
  - ion temperature maximum scales with density peaking factor

N. Pablant, NF **60** (2020)

The Phase-Contrast Imaging diagnostic

E. M. Edlund, et al, Rev. Sci. Instr. 89, 10E105 (2018)

- PCI measures line-integrated density fluctuations along the CO_2 laser beam path with 32 chords,

$$I = \int \tilde{n}\,\mathrm{dl}$$

- Measures combination of k_θ and k_ρ with a small radial component on the outboard side

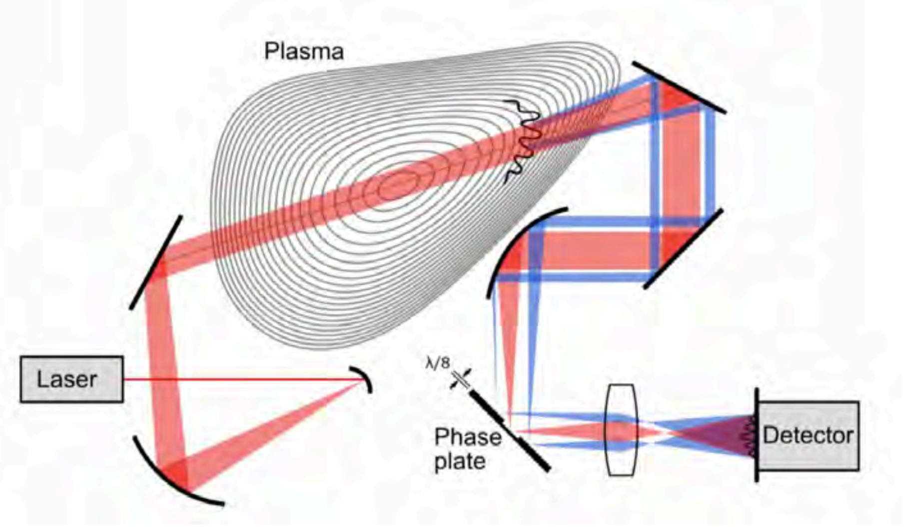

Instability	$k_\theta\rho$	k_θ [cm^{-1}]
ITG	0.1	0.3
TEM	1	2.8
ETG	10	27

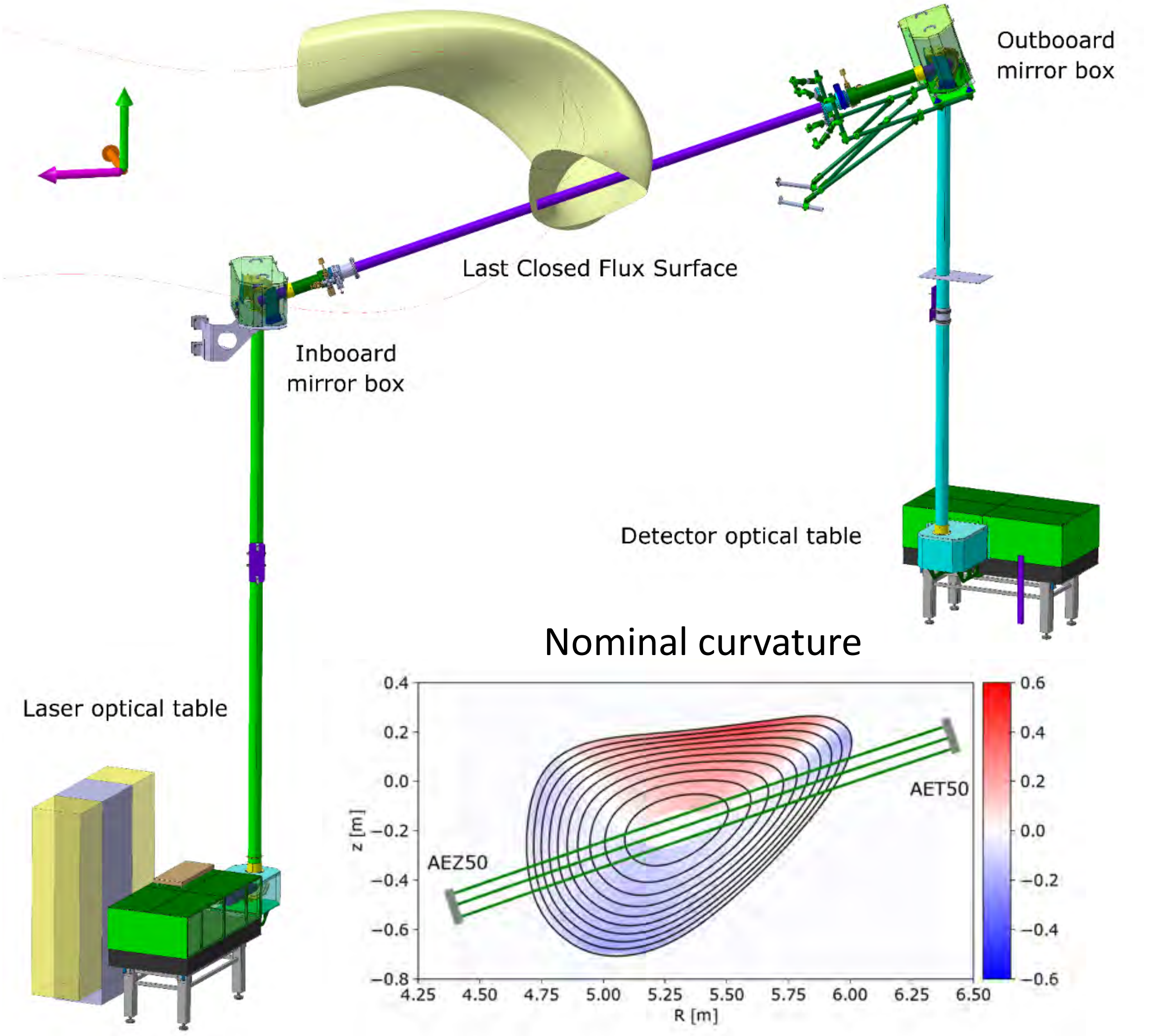

PCI Operation Principle

C. Rost et al, TP15.00017 at this meeting

Beam traversing plasma, acquires time/space dependent phase shift $\Delta\phi(x,t) \propto \int \tilde{n}_e(x,y,t)dy$

- $E_{\text{pl}} = E_0 e^{i\Delta\phi} \simeq E_0(1 + i\Delta\phi)$, $I \propto |E_{\text{pl}}|^2 = |E_0|^2$
- Phase plate adds path length, phase of central component
- $E_{\text{det}} = E_0(i + i\Delta\phi)$, $|E_{\text{det}}|^2 = |E_0|^2(1 + 2\Delta\phi)$

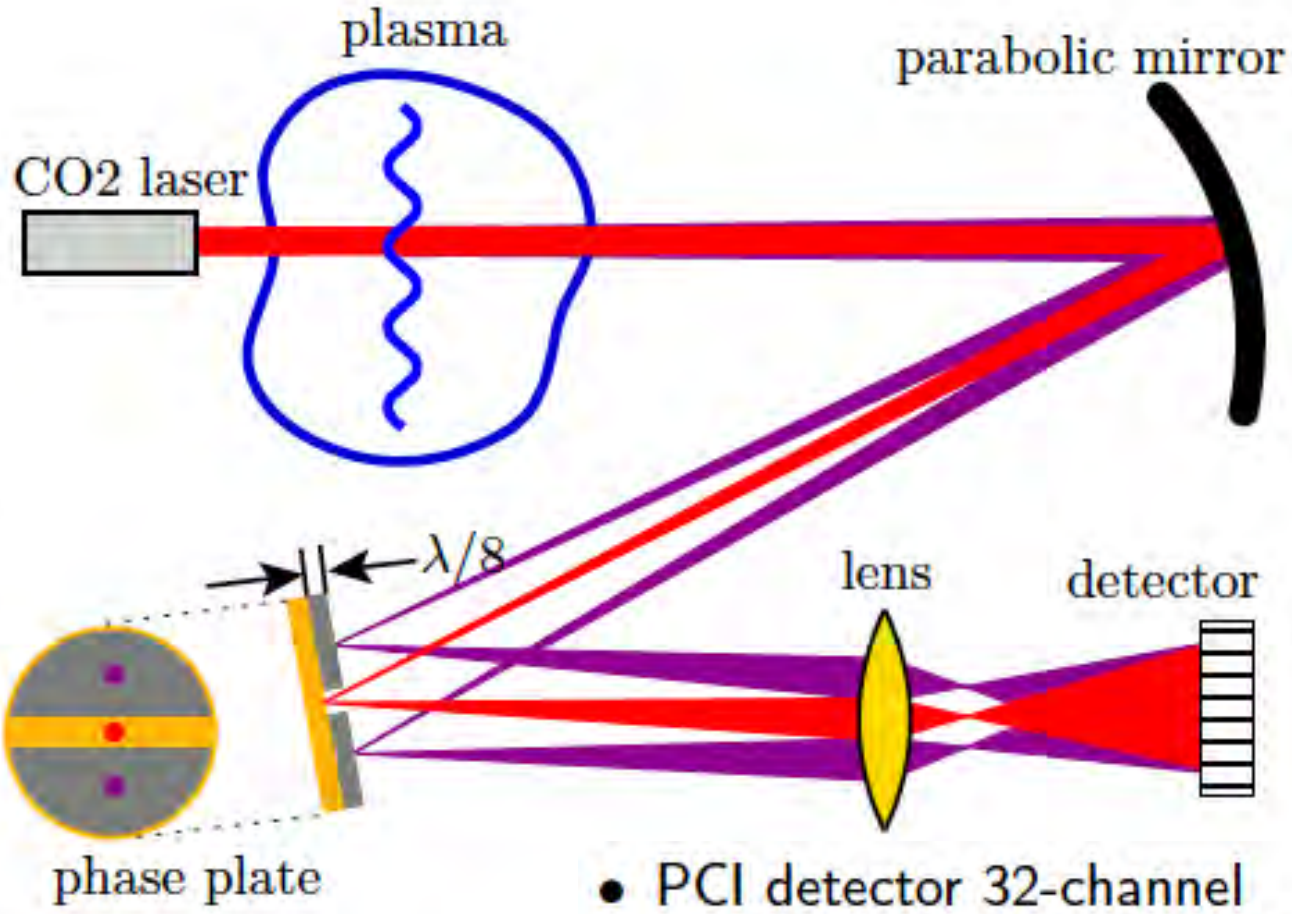

- PCI detector 32-channel HgCdTe with $\Delta f = 2\,\text{MHz}$

Wave number range: $1 < k < 30\,\text{cm}^{-1}$

Ion temperature profiles in gas-fueled ECRH discharges show little variation with density

density profiles

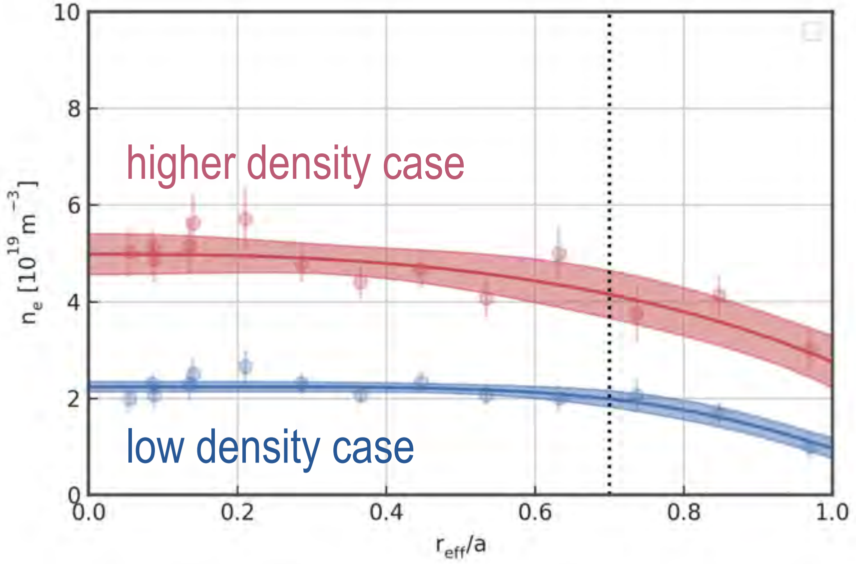

a/L_n (r/a=0.7) = 0.6 ± 0.2 → 0.5 ± 0.1

electron/ion temperature profiles

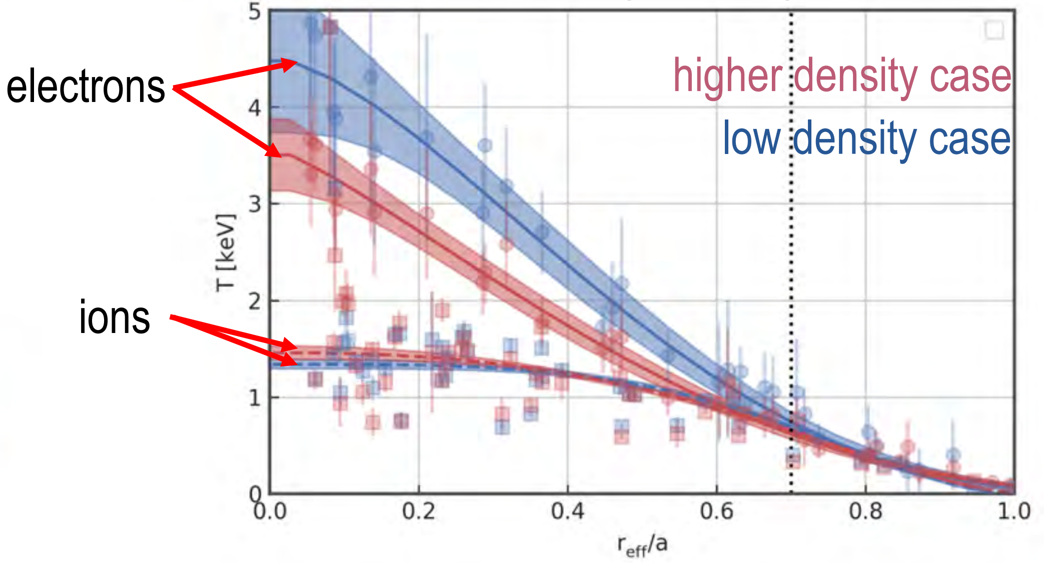

$a/L_{Ti} \approx a/L_{Te}$ (r/a=0.7) = 3.3 ± 0.5 → 2.8 ± 0.3

- The n_e and T_e profiles are self-similar across many different experimental situations.
- Ion temperature profiles are "clamped" in the core at about 1.6 keV despite significant increases in density.
- The normalized gradient scale lengths for ions and electrons are comparable for both density and temperature.

PCI density fluctuations in flat density ECRH discharges show changes in ExB velocity

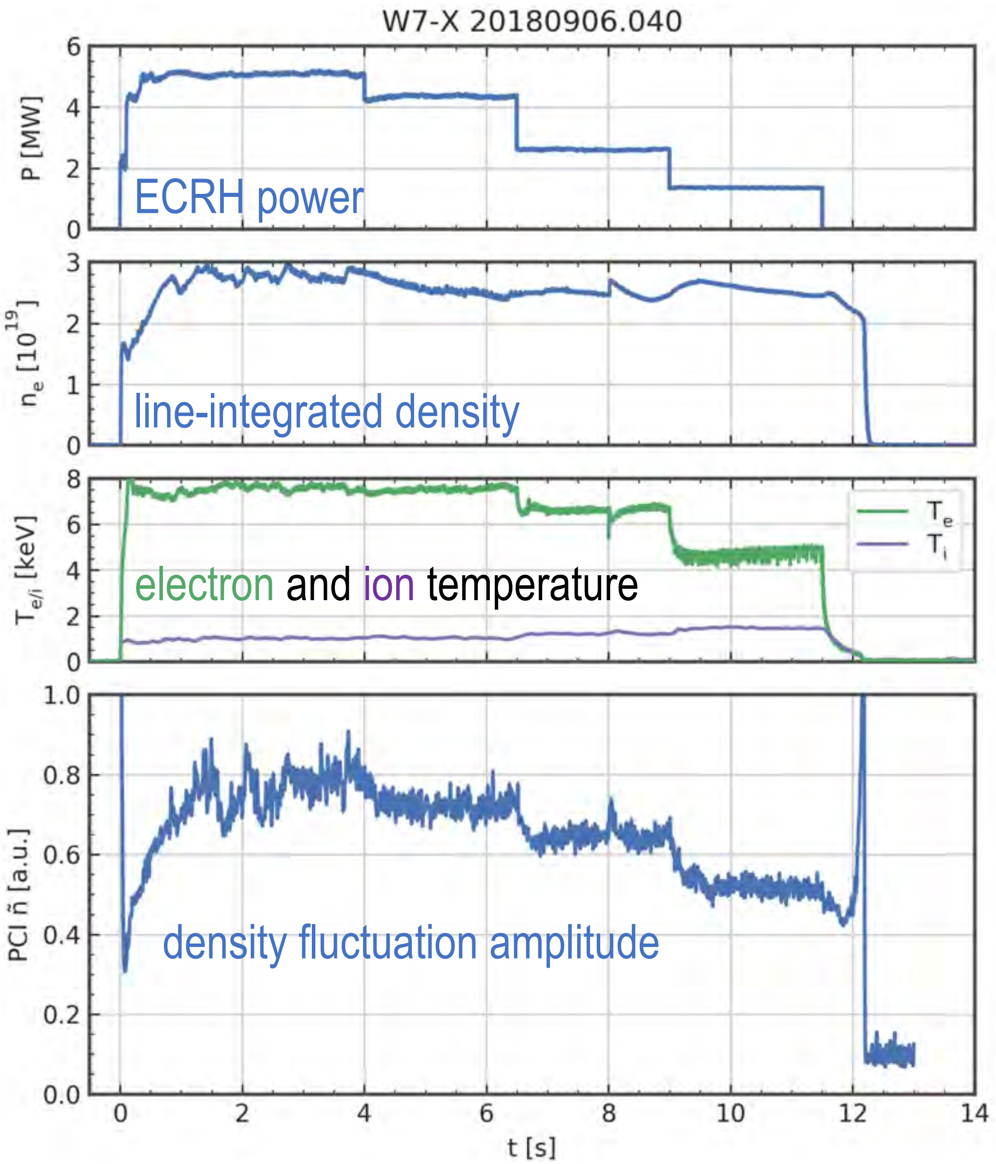

normalized frequency-wavenumber spectra S(k,f)

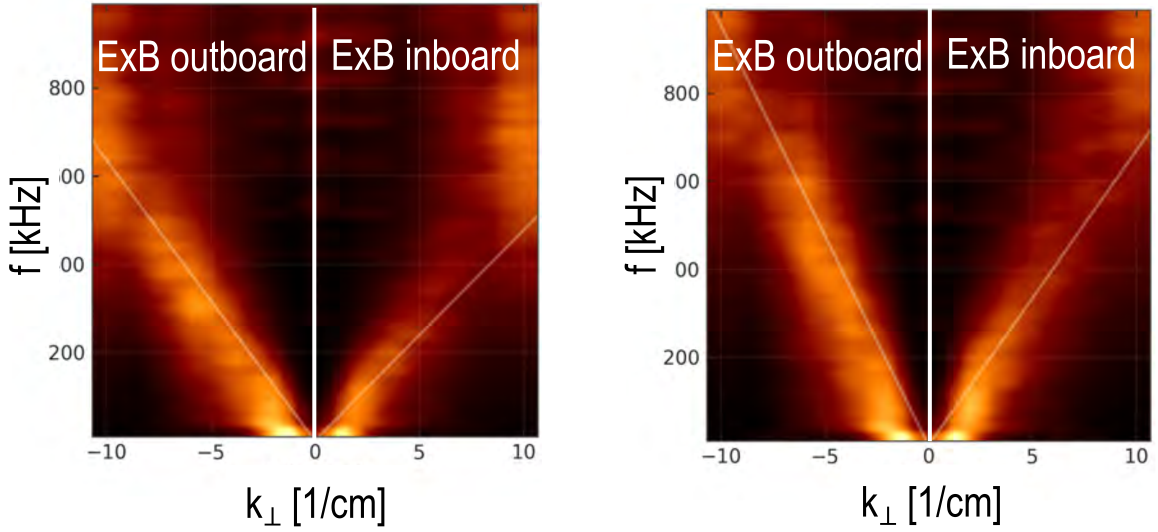

- Fluctuations scale with input power and T_e, by extension W_{dia}
- k-spectra virtually unmodified across parameter space
- Single phase velocity, varies with local E_r

Pellet fueling produces substantial changes in density and ion temperature profiles

density profiles

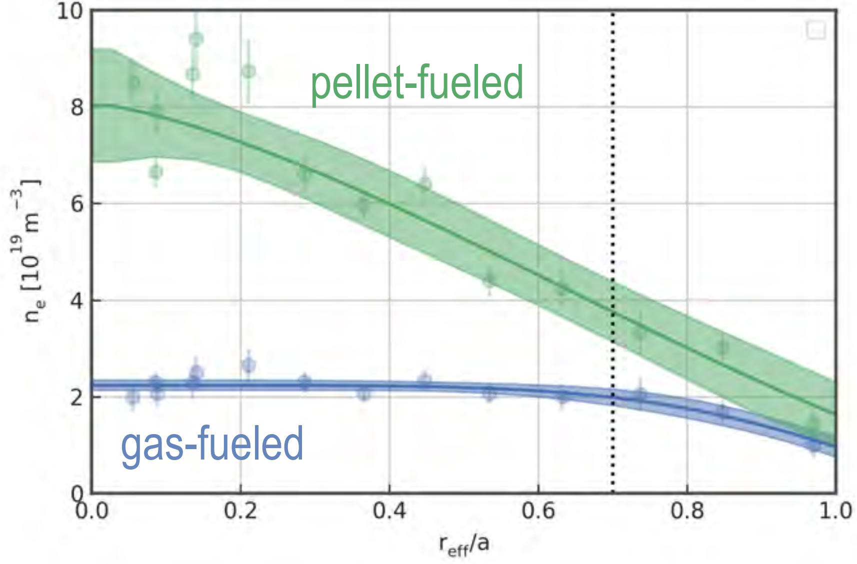

a/L_n (r/a=0.7) = 0.6 ± 0.2 → 1.3 ± 0.4

electron/ion temperature profiles

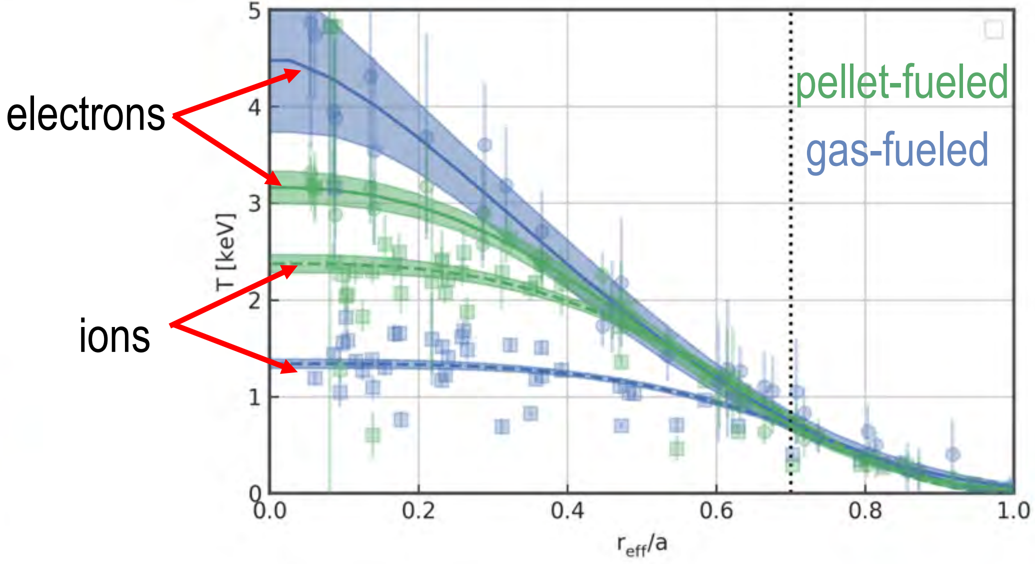

$a/L_{Ti} \approx a/L_{Te}$ (r/a=0.7) = 3.2 ± 0.5 → 3.7 ± 0.5

- After pellet fueling: significant density gradients extend far into core
- Ion temperature profile coupled to electron temperature, $T_e=T_i$ for r/a > 0.5

Baldzhun et al, PPCF 61, 095012 (2019).

Density fluctuations in pellet fueled discharges

A. von Stechow, et al, submitted to PRL, 2020

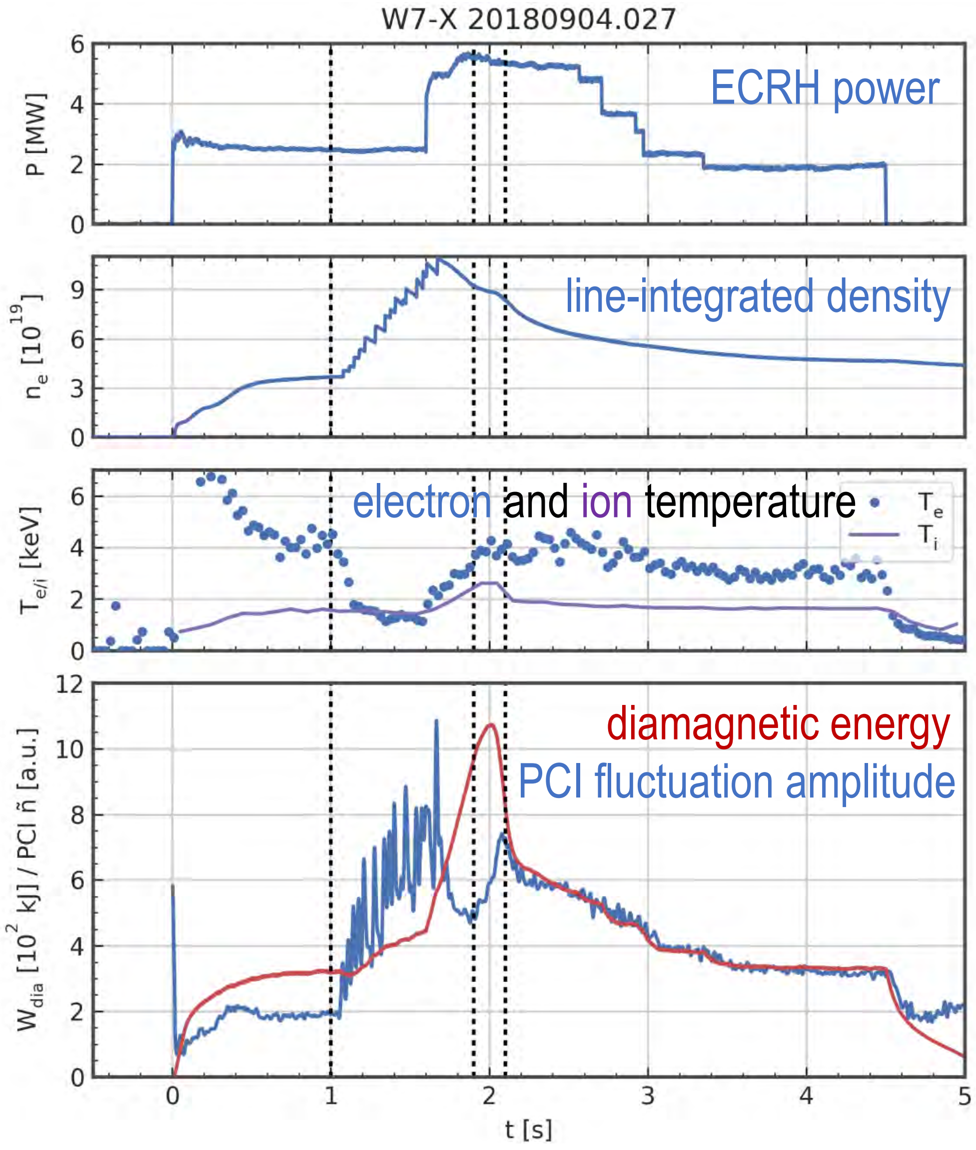

normalized frequency-wavenumber spectra

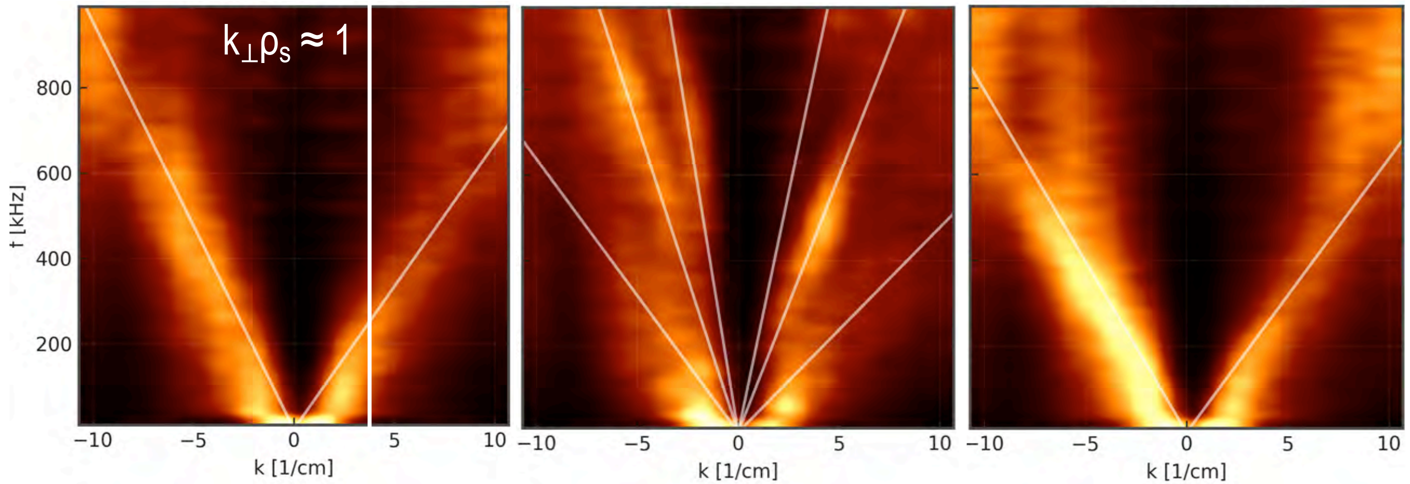

before pellets (1.0s)

after pellets (1.9s)

after W_{dia} drop (2.1s)

- Rapid increase in W_{dia} observed after pellet injection (together with T_e, T_i)
- PCI **fluctuation amplitude significantly reduced** during W_{dia} increase
- During reduced fluctuation phase: **multiple phase velocities observed**
- Regular fluctuations and k-f-spectra recovered during W_{dia} drop

Profile shaping by neutral beam injection

- See talk by Z. Huang at this conference: MF1-05; also impact of ECH

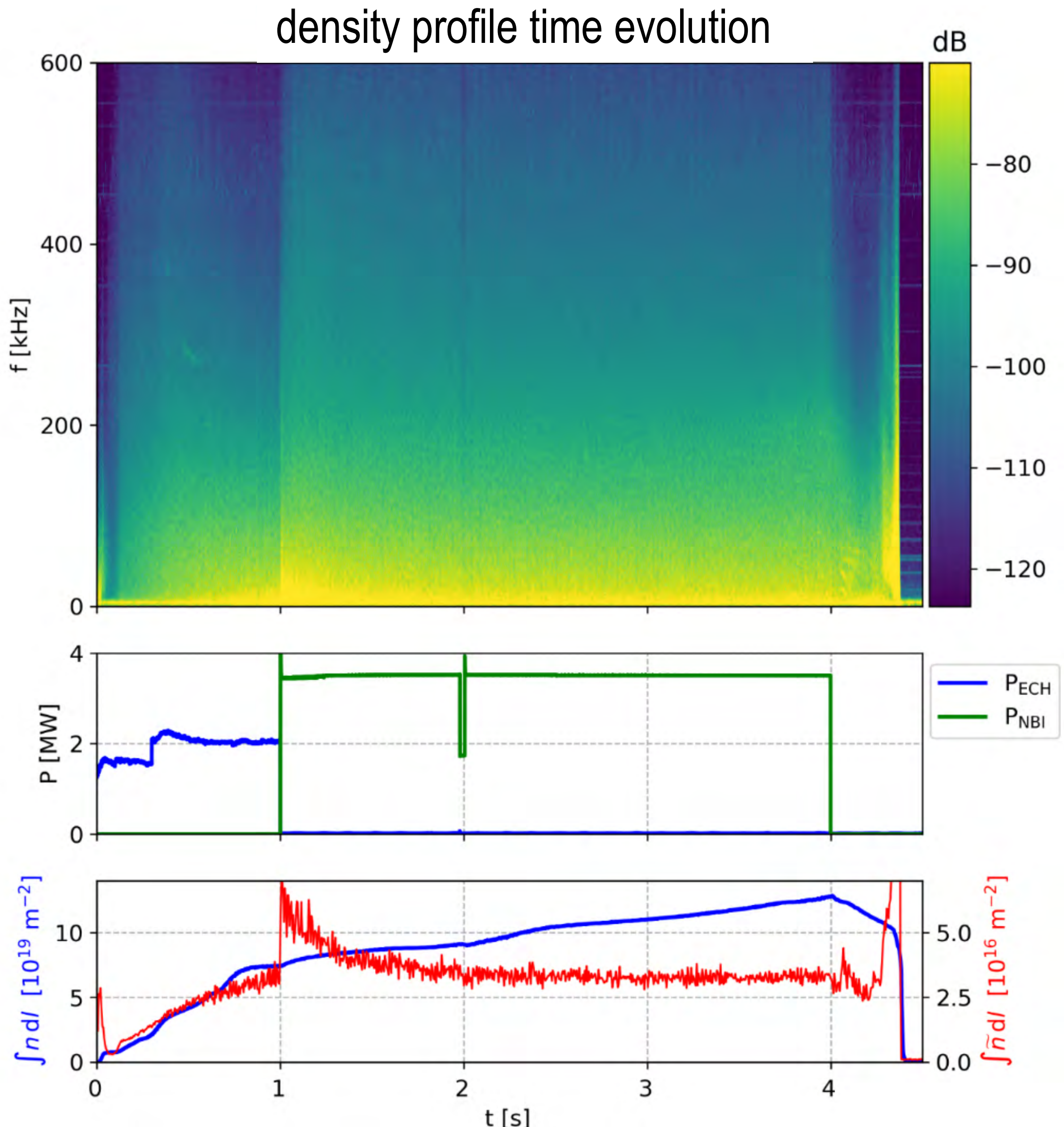

[Z. Huang]

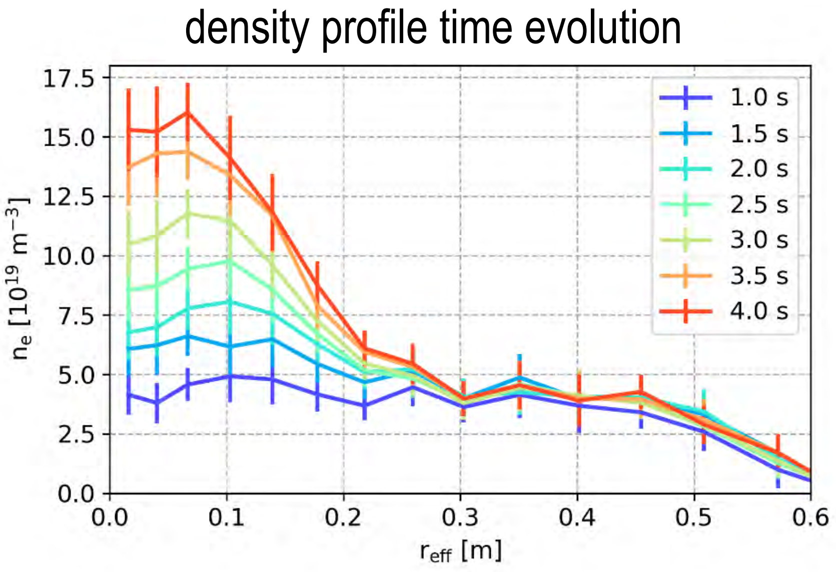

- Pure NBI discharges achieve **density peaking far in the core**
- Density profile outside half radius unaffected
- PCI **fluctuations virtually unaffected** (amplitude and spectra)
- **Core density gradient:**
  1. **does not stabilize existing instabilities**
  2. **does not drive additional instabilities**

Gyrokinetic simulations with GENE: linear stability maps

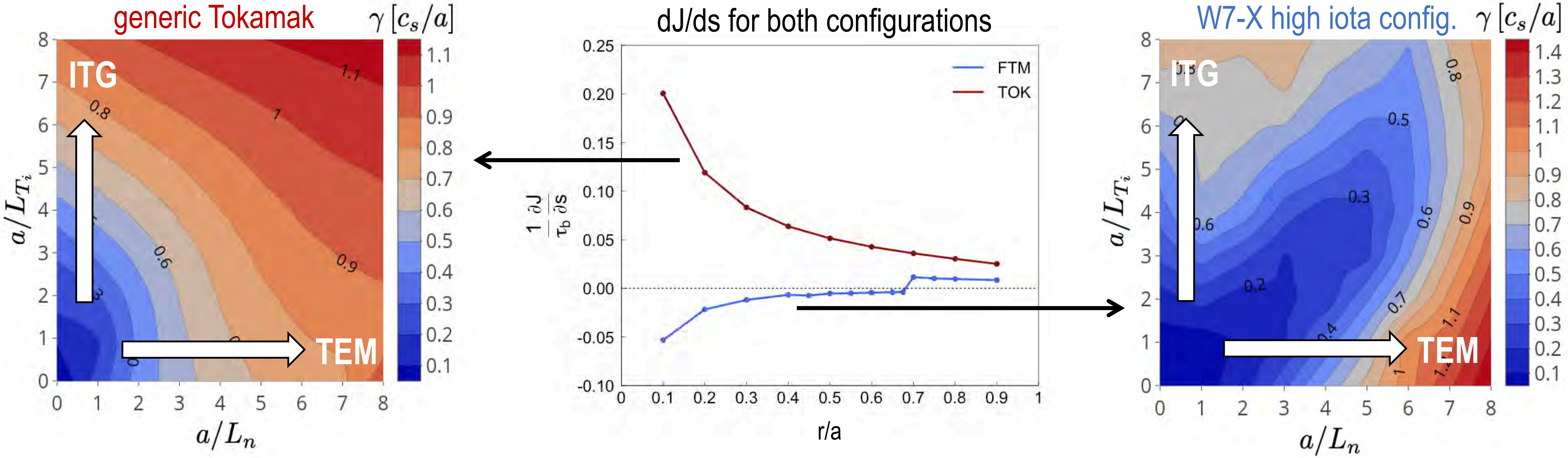

- Linear GENE runs for a large set of ∇T and ∇n in different magnetic geometries (w/ $T_i=T_e$, $E_r=0$, $\beta=0$)
  Alcusón, Xanthopoulos *et al.*, PPCF 62 (2020)
- W7-X: stability "valley" where $a/L_T \approx a/L_n$
- Gyrokinetic model: Stabilty region for W7-X derives from maximum-J property: $dJ/ds < 0$
  Proll *et al.*, Phys. Rev. Lett. 108 (2012) and Plunk *et al.*, J. Plasma Phys. 83 (2017).
- With max-J: (1) ITG stabilizes quickly with ∇n and (2) TEM responds weakly to ∇n

Alfven waves are observed under many conditions

- Alfven waves have been observed in both ECH-only and NBI heated plasmas.
- The measured spatial structures for these modes observed by PCI exhibits the characteristic multi-peaked structure characteristic of coherent, large–scale structures.

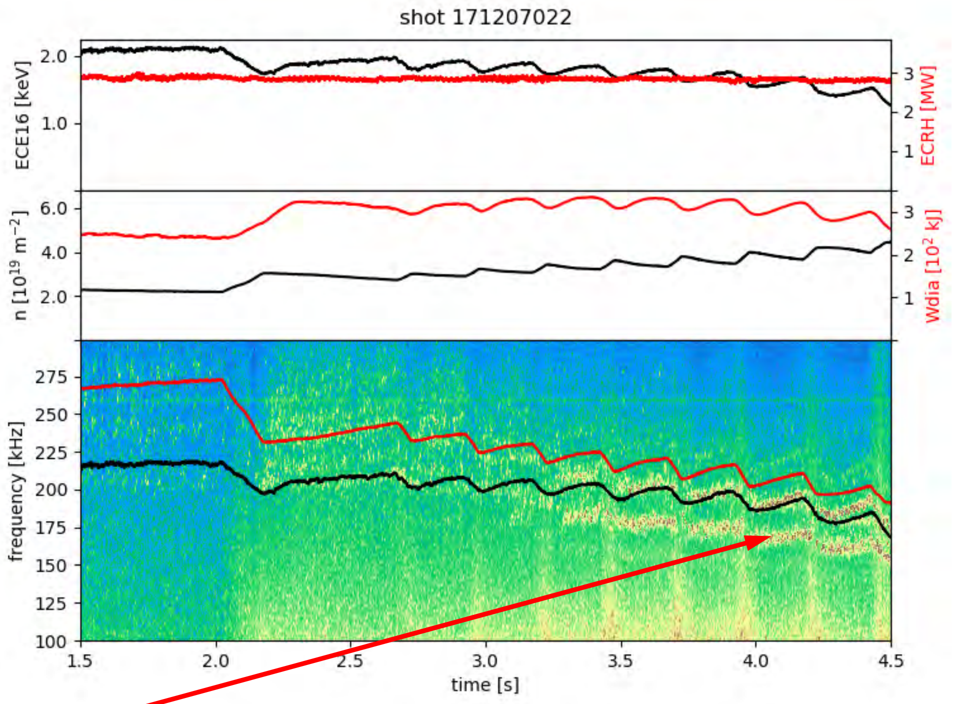

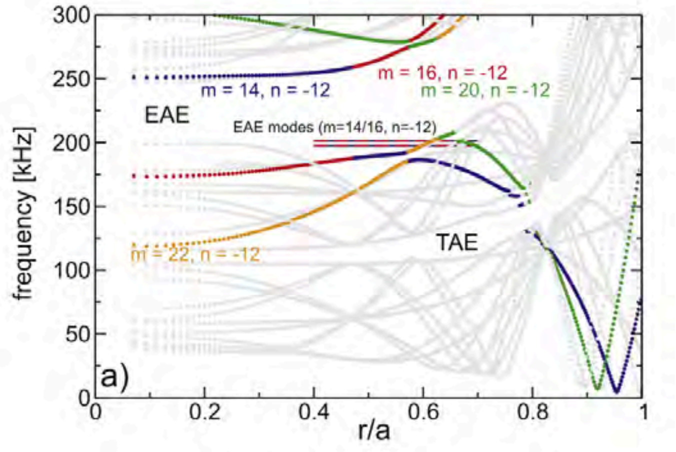

Windisch *et al.*, PPCF **59**, 105002 (2017).

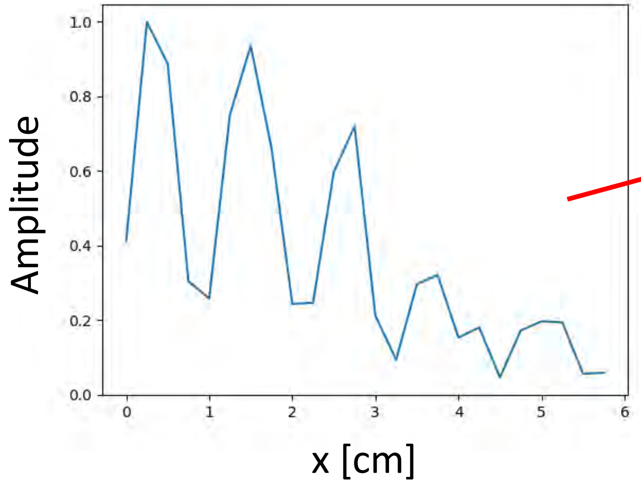

Alfvén waves observed during a series of pellet injections that caused the density to increase.

The red trace is the Alfvén frequency, based on the mean density, and the black trace is $\sqrt{T_e}$.

Plans for 2020 upgrades

- New CO_2 laser:
    - Manufacturer: Access Laser (Everett, WA)
    - Model: AL20, water cooled
    - Output power: 20 Watts, with line tracker
- New torus hall beam lines
- Implement rotating masks for wavenumber filtering (radial localization)
- Optical heterodyne detection system (in development)
    - ICRH waves in 2-ion and 3-ion plasmas at 25 MHz and 38 MHz

      Kazakov *et al.*, NF **55**, 032001 (2015).

      Tsujii *et al.*, PoP **22**, 082502 (2015).
    - Ion-cyclotron emission (ICE) at harmonics of ion cyclotron frequencies

      Dendy *et al.*, PPCF **57**, 044002 (2015).

      Carbajal *et al.*, PoP **21**, 012106 (2014).

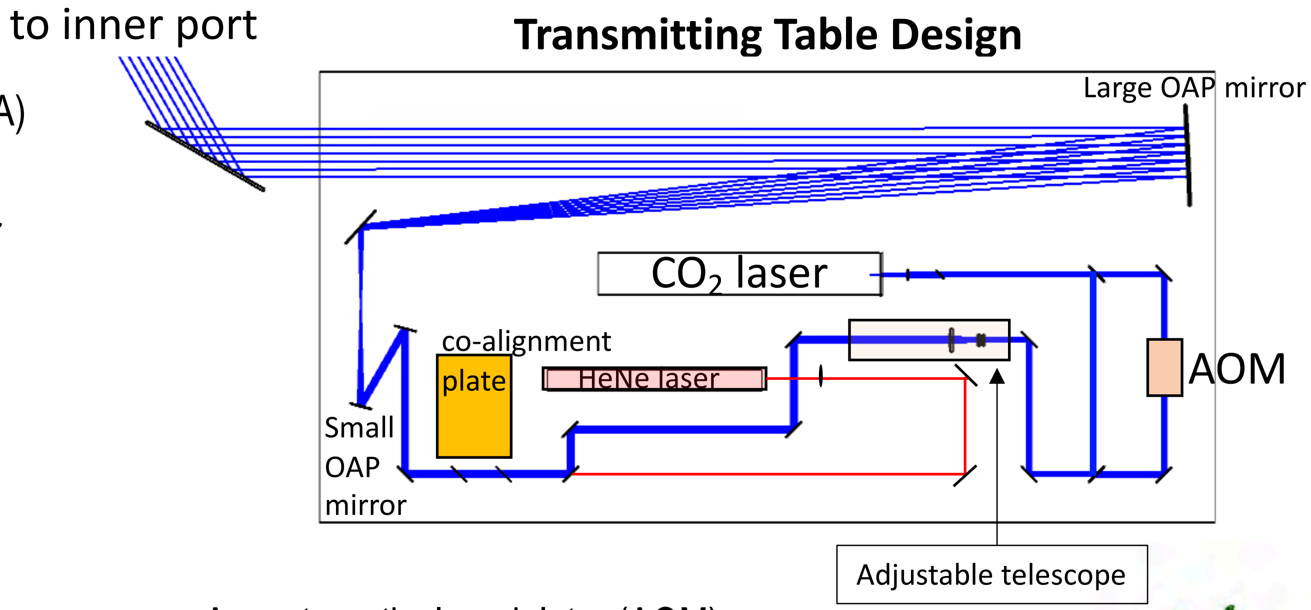
Transmitting Table Design

- Acousto-optical modulator (AOM)
- Input power: 55 Watts (typical)
- Center frequency: 30 MHz

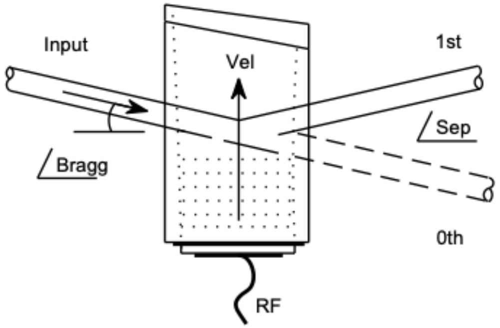

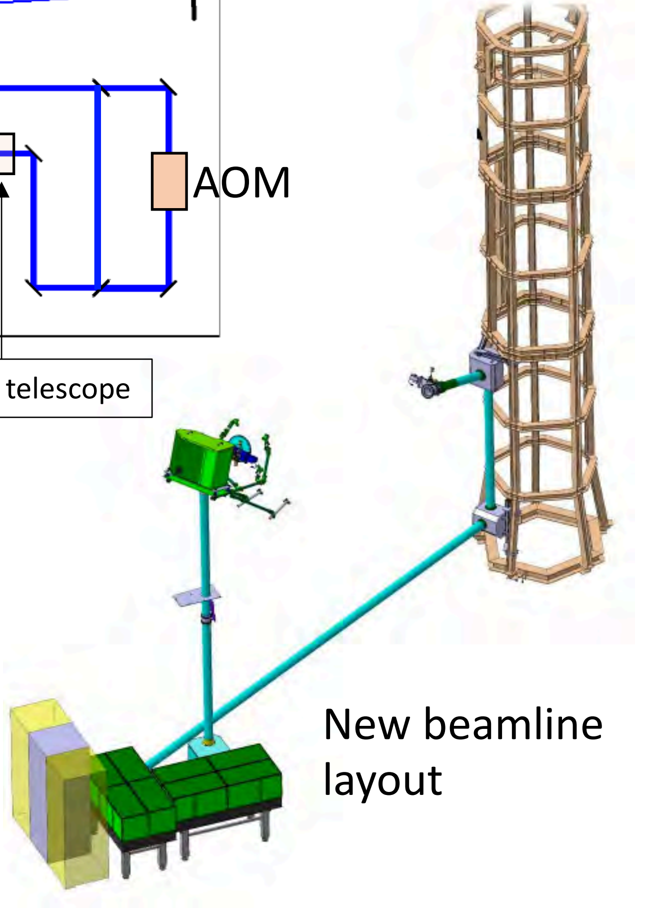
New beamline layout

Conclusions and Summary

- Phase Contrast Imaging (PCI) has been implemented on W7-X and has measured:
  - Turbulence under a wide range of conditions, where the phase velocity of the turbulent fluctuations is dominated by the measured ExB velocity
  - Alfven eigenmodes have been detected in both purely ECH and NBI heated discharges
- The ion heat flux has been reduced to neoclassical levels by peaking the profiles with pellet fueling in ECH driven discharges, consistent with the reduced level of turbulence measured with PCI
- Nonlinear GK runs confirm that the ion heat flux is strongly reduced in the “stability valley” and the electric field further limits ITG growth (Xanthopoulos et al, PRL, 2020)
- In combination with 3D GENE simulations, a synthetic PCI analysis is being developed for OP2 to compare code predictions quantitatively with PCI measurements